

Oil & Natural Gas Technology

DOE Award No.: DE-FE0028895

Quarterly Research Performance Progress Report (Period ending 12/31/2016)

Dynamic Behavior of Natural Seep Vents: Analysis of Field and Laboratory Observations and Modeling

Project Period (10/01/2016 to 09/30/2017)

Submitted by:
Scott A. Socolofsky



Texas A&M Engineering Experiment Station
DUNS #:847205572.
3136 TAMU
College Station, TX 77843-3136
e-mail: socolofs@tamu.edu
Phone number: (979) 845-4517

Prepared for:
United States Department of Energy
National Energy Technology Laboratory

January 31, 2017



Office of Fossil Energy

DISCLAIMER:

This report was prepared as an account of work sponsored by an agency of the United States Government. Neither the United States Government nor any agency thereof, nor any of their employees, makes any warranty, express or implied, or assumes any legal liability or responsibility for the accuracy, completeness, or usefulness of any information, apparatus, product, or process disclosed, or represents that its use would not infringe privately owned rights. Reference herein to any specific commercial product, process, or service by trade name, trademark, manufacturer, or otherwise does not necessarily constitute or imply its endorsement, recommendation, or favoring by the United States Government or any agency thereof. The views and opinions of authors expressed herein do not necessarily state or reflect those of the United States Government or any agency thereof.

Contents

1 Accomplishments	5
1.1 Summary of Progress Toward Project Objectives	5
1.2 Progress on Research Tasks	6
1.2.1 Task 1.0: Project Management Planning	6
1.2.2 Task 2.0: Analyze NETL Water Tunnel Data	7
1.2.3 Task 3.0: Synthesize GISR Field Data	7
1.3 Deliverables	17
1.4 Milestones Log	17
1.5 Plans for the Next Reporting Period	17
2 Products	20
2.1 Publications, Conference Papers, and Presentations	20
2.2 Websites or Other Internet Sites	20
2.3 Technologies or Techniques	20
2.4 Inventions, Patent Applications, and/or Licenses	20
2.5 Other Products	20
3 Participants and other collaborating organizations	20
3.1 Project Personnel	20
3.2 Partner Organizations	21
3.3 External Collaborators or Contacts	21
4 Impact	21
5 Changes / Problems	21
6 Special Reporting Requirements	23
7 Budgetary Information	23

List of Figures

1 Project Timeline.	6
-----------------------------	---

2	Volumetric bubble size distribution for the measured data and a fitted log-normal distribution. Left panel: cumulative distribution function; right panel: probability distribution function.	8
3	Measured rise velocity versus bubble size. Errorbars show the standard deviation of instantaneous rise velocity data.	9
4	Cumulative distribution function of bubble size by volume in the water column. . . .	10
5	Image of the natural seep flare in the water column from post-processed EM-302 data together with the measured temperature profile and hydrate stability curve. . .	11
6	Two sample images recorded by the M3 Sonar during the GISR G08 Cruise. Upper panel: altitude 90 m; lower panel: altitude 190 m. The range for image plotted in both panels is 20 m.	12
7	Width of seep flare plume from the M3 sonar for dive H1402. Measurement data were obtained from 50 Sonar images with errorbars reporting the standard deviation of the data. Model results from TAMOC for different lateral diffusivities are plotted, showing plume width given as 2σ , where σ is the standard deviation of modeled bubble locations at each altitude.	13
8	Comparison of bubble spreading between the model and measurements for all dives in G08. $K_a = 3 \times 10^{-4} \text{ m}^2/\text{s}$ is used in all simulations.	14
9	Comparison between the measured M3 sonar image (left column) and the target strength map created from the model result (right column).	15
10	Left panel: 3-D scatter plot of unspecified amplitude from the EM-302 after noise removal, illustrating the location and magnitude of seep bubbles; right panel: comparison between the modeled target strength and the measured unspecified amplitude, where errorbars present standard deviation of the data, and dashed line shows the obtained noise level below which all data points were removed in the scatter plot. The model profile is offset by 17 dB to match the location of measured unspecified amplitude.	16

List of Tables

1	Milestones schedule and verification methods.	18
2	Budget Report	24

1 Accomplishments

1.1 Summary of Progress Toward Project Objectives

The *overarching goal* of this project is to develop a computer model to predict the trajectory and dissolution of hydrate-armored methane bubbles originating from natural seeps. The model is based on the Texas A&M Oilspill Calculator (TAMOC), developed by Dr. Socolofsky, and which will be refined and validated through this project to explain fundamental laboratory and field observation of methane bubbles within the gas hydrate stability zone of the ocean water column. *Our approach* is to synthesize fundamental observations from the National Energy Technology Laboratory's (NETL) High-Pressure Water Tunnel (HPWT) and field observations from the Gulf Integrated Spill Research (GISR) seep cruises (cruises G07 and G08), conducted by the PIs in the Gulf of Mexico, to determine the dissolution pathways and mass transfer rates of natural gas bubbles dissolving in the deep ocean water column. We will achieve these objectives by pursuing the *following specific objectives*:

1. Analyze existing data from the NETL HPWT.
2. Synthesize data from the GISR natural seep cruises.
3. Refine and validate the seep model to predict available data.
4. Demonstrate the capability of the seep model to interpret multibeam data.

Ultimately, the *main outcome and benefit* of this work will be to clarify the processes by which hydrate-coated methane bubbles rise and dissolve into the ocean water column, which is important to predict the fate of methane in the water column, to understand the global carbon cycle, and to understand how gas hydrate deposits are maintained and evolve within geologic and oceanic systems, both at present baselines and under climate-driven warming.

The work accomplished during this reporting period focused on the first two specific objectives. To begin analysis of the HPWT data, we have worked to transfer all of the data (about 30 TB) from NETL to a new server installed at Texas A&M University. For the GISR field data, we have worked intensively to complete post-processing of the image data collected during the G08 cruise (data from the G07 cruise has been analyzed previously and was reported in Wang et al. 2016) and to begin development of the analysis tools for the acoustic data collected during each of these cruises (G07 and G08).

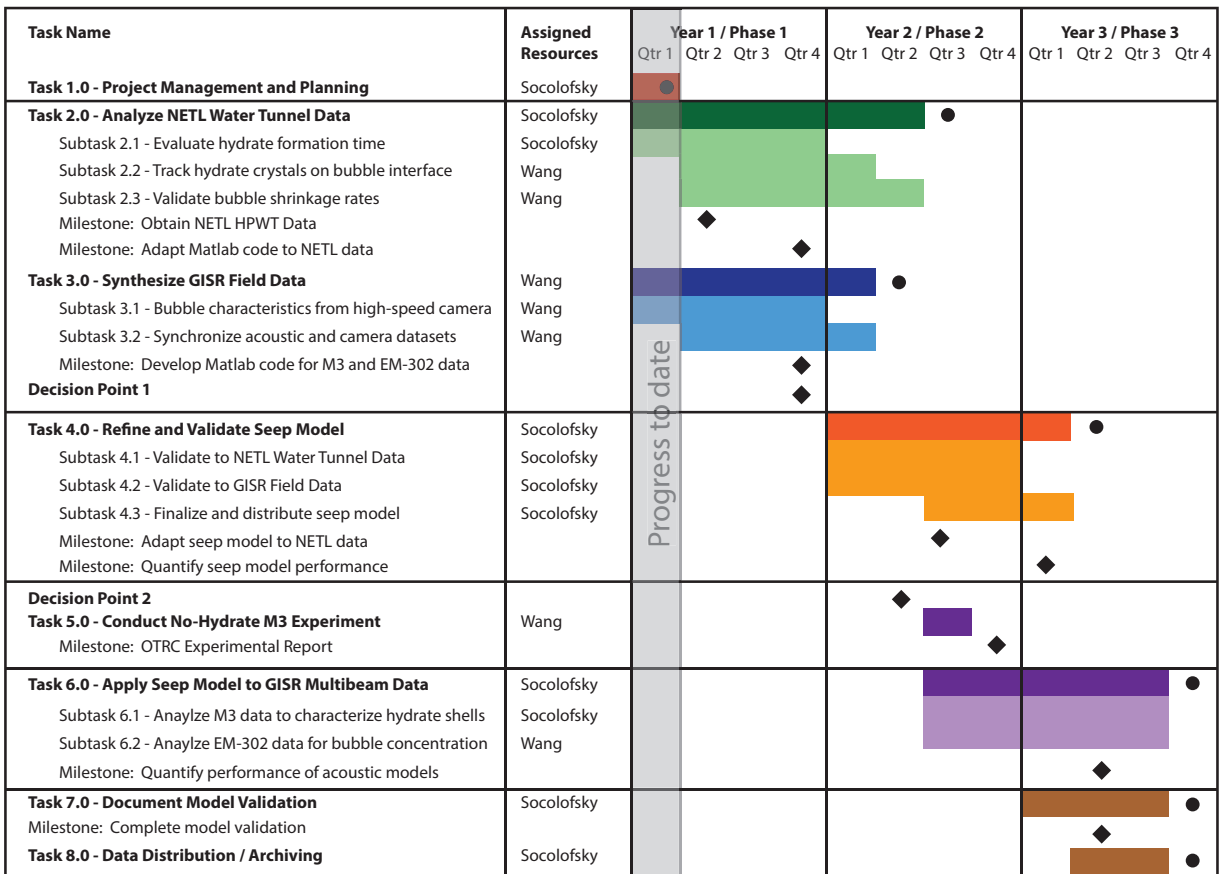


Figure 1: Project Timeline.

1.2 Progress on Research Tasks

Figure 1 presents the project timeline, showing each of the project tasks, subtasks, and milestones as identified in the Project Management Plan (PMP). The present reporting period concludes the first quarter of FY 2017 (Phase 1 of the project). During this period, Task 1 was completed, and Tasks 2 and 3 were initiated. The work conducted on these tasks during this reporting period is summarized in the following sections, organized by each Task.

1.2.1 Task 1.0: Project Management Planning

Preparation of the PMP was initiated as soon as the notice of award was received. After iteration with the project manager, the PMP was accepted as of October 28, 2016. The PMP will be updated as necessary throughout the project as required by the Project Officer.

1.2.2 Task 2.0: Analyze NETL Water Tunnel Data

The first step in analyzing the NETL water tunnel data is to obtain a complete copy of the original image files. This action was initiated as soon as the notice of funding was received. We coordinated with the current NETL curator of the data, Franklin Shaffer, and the NETL data library. The data usage agreement was completed quickly, and allows us to have a complete copy of the data at Texas A&M, to analyze the data, and to report on results of our analysis in public journals. The only restriction is that we should not provide public access to the data or give the data to anyone outside the project without NETL approval.

To archive the data at Texas A&M University, we purchased a network storage device, as planned in the project budget. The storage device is installed on our internal University network, and access is restricted to users with authorized accounts. Currently, there are accounts for Franklin Shaffer, the Texas A&M IT Department, and for the two project PIs (Socolofsky and Wang).

Following approval of our data usage agreement and installation of the network storage, we began to transfer the data. Our initial attempts were to pass the data over the internet via FTP. While establishing an FTP connection was successful, data transfer rates were limited on the NETL upload side such that transfer would be prohibitively long. At that point, Franklin Shaffer copied all of the data over to a bundle of 3 TB hard drives and shipped these drives to Texas A&M University. Copying of the data is currently underway and will continue into the second quarter reporting period. We anticipate the complete dataset will be copied to our server by the end of January 2017, on schedule for the first project Milestone.

1.2.3 Task 3.0: Synthesize GISR Field Data

The project PIs conducted two research cruises to natural seeps in the Gulf of Mexico under funding to the GISR consortium. These were the G07 cruise in July 2014 to Mississippi Canyon (MC) block 118 and to Green Canyon (GC) block 600 and the G08 cruise in April 2015 to MC 118. Both cruises were on the *E/V Nautilus* and utilized the remotely operated vehicle (ROV) *Hercules*. This project utilizes two main datasets from these cruises: data from our stereoscopic high-speed camera system mounted on the ROV (Wang et al. 2015) and acoustic data collected by an M3 sonar mounted on the ROV and an EM-302 multibeam sonar mounted on the haul of the ship. The image data from the G07 cruise was analyzed previously and reported in Wang et al. (2016). This project will analyze all of the acoustic data and complete analysis of the image data for the

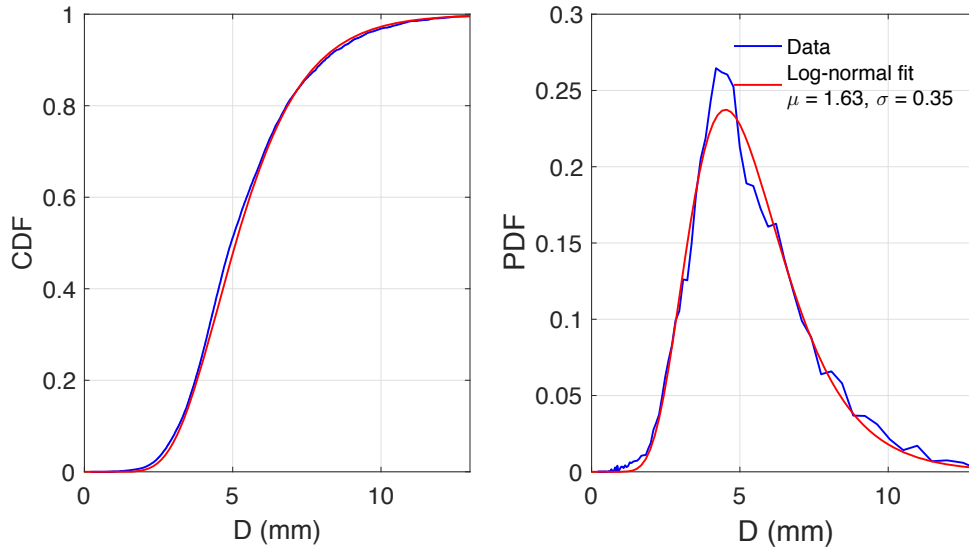


Figure 2: Volumetric bubble size distribution for the measured data and a fitted log-normal distribution. Left panel: cumulative distribution function; right panel: probability distribution function.

G08 cruise.

Subtask 3.1 - Bubble Characteristics from High-Speed Camera. During the present reporting period, we analyzed the G08 image data for bubble size and rise velocity. We collected data at the seafloor and at several elevations up the water column to a maximum height of 400 m above the seafloor (490 water depth).

During the G08 cruise, the source of bubbles at the seafloor was distributed over a region several 10's of square meters in area, and was quite unsteady both in flow rate and specific source location throughout the cruise. Hence, to sample the source, the ROV made several transects through the plume with the cameras recording along the transects. Some data was also collected for stationary measurements at major venting areas. Figure 2 shows the bubble size distribution from our image analysis of all of the data collected at the source. The volume median bubble size was about 5 mm, and the data fit very well to a log-normal distribution.

For the G07 cruise, many of the bubbles sampled at the source rose at rates slower than predicted by empirical equations based on laboratory experiments (e.g., correlations in Clift et al. 1978). We were able to show in Wang et al. (2016) that these slower-rising bubbles had zig-zag trajectories that lied in a two-dimensional plane and that bubbles rising at the faster rates predicted by the empirical equations have helical paths that are three-dimensional. Our analysis of the G08 data show that the bubbles during this cruise more consistently match the expected empirical equations.

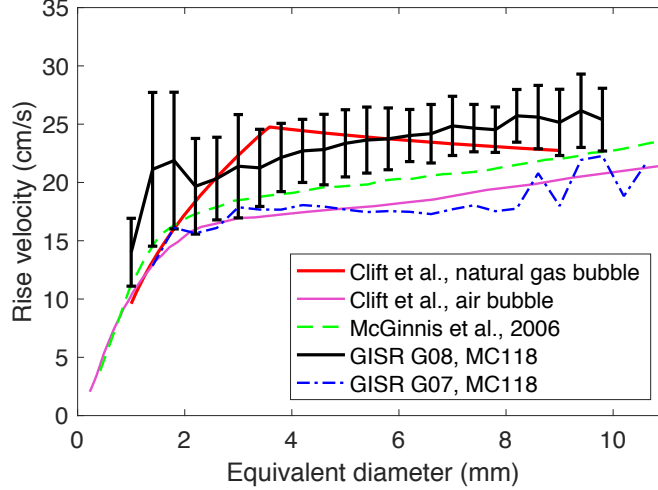


Figure 3: Measured rise velocity versus bubble size. Errorbars show the standard deviation of instantaneous rise velocity data.

Figure 3 shows the statistics of the data analyzed for G08 (black curve and error bars) together with the empirical predictions (red line) and data for our G07 cruise. The bubbles for the G08 cruise are consistently faster than for G07. The main difference in the release conditions during G08 compared to G07 that might explain this different rise velocity is that during the G08 cruise the bubble source was percolating up through the sediments and was quite variable in space and in flow rate. During G07, all of the sources were very stable, emanated from established channels through fixed points in the seafloor and at relatively constant flow rates. Perhaps these fixed channels favored initial conditions that give rise to the slower, zig-zag rising paths.

We also collected image data at several heights above the seafloor to document the evolution of the size distribution with height. Ambient currents act to segregate the bubbles by size, with larger bubbles rising at steeper angles through the water column than smaller bubbles, which are advected more noticeably downstream. At each height, we used the M3 sonar to track the bubble flare and collected image samples at the location in the M3 image where the acoustic backscatter appeared greatest. Figure 4 presents our analysis of the cumulative distribution of bubble size by volume for each height sampled during the G08 cruise. It is evident from the data that 1.) the volume median bubble size decreases with height and 2.) that the distribution of bubble sizes becomes narrower with height, which supports our observation that the currents acted to sort the bubbles by size. The decrease in the volume median bubble size is not monotonic with height. This is another artifact of the fact that we have limited sample size in a flare that is being sorted by the currents.

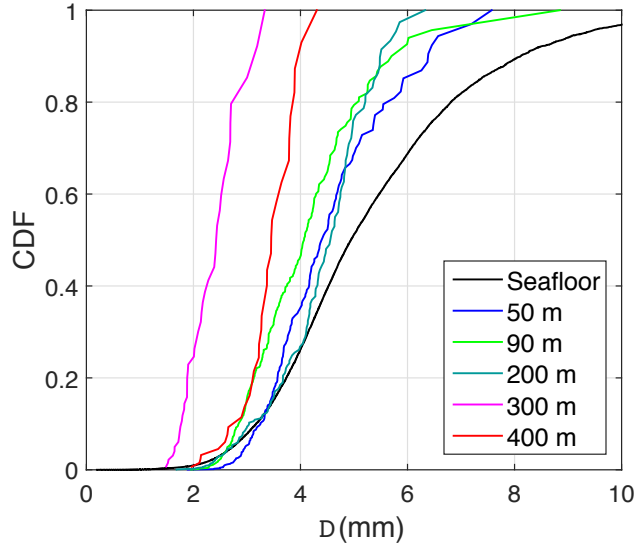


Figure 4: Cumulative distribution function of bubble size by volume in the water column.

Each of these figures summarizes the large dataset of instantaneous data contained in our post-processed dataset and helps to show the main conclusions given by the data. We will work in the coming quarter to build a database to contain the post-processed data, and the final deliverable for Task 3 will include the complete dataset of instantaneous measurements.

Subtask 3.2 - Synchronize Acoustic and Camera Datasets.

Work for this task during the present reporting period focused on extracting the acoustic data, cataloging the data by time stamp so that it can be synchronized with the image data, and developing new analysis tools to extract bubble characteristics from the image data.

Figure 5 shows a post-processed image from the EM-302 haul-mounted multibeam of the MC 118 seep flare during the G08 cruise. The large plume source at the origin of the superposed graph is the source sampled during this cruise. As shown in the figure, most of the flare signal is below the hydrate stability line.

Figure 6 shows a sample of the data recorded by the M3 sonar mounted on the ROV. The M3 multibeam sonar was mounted with a horizontal orientation, looking ahead of the ROV and slightly up at about a 3° angle. Thus, acoustic images present cross-sections through the bubble flare. The upper image is closer to the seafloor, showing the extent of the distributed source coming up from the sediments (the image range is 20 m in the figure). The lower image is from 100 m higher in the water column. At that height, smaller bubbles have dissolved or have been advected away from the main flare by the currents. Also, the intermittency of the source conditions was unsteady

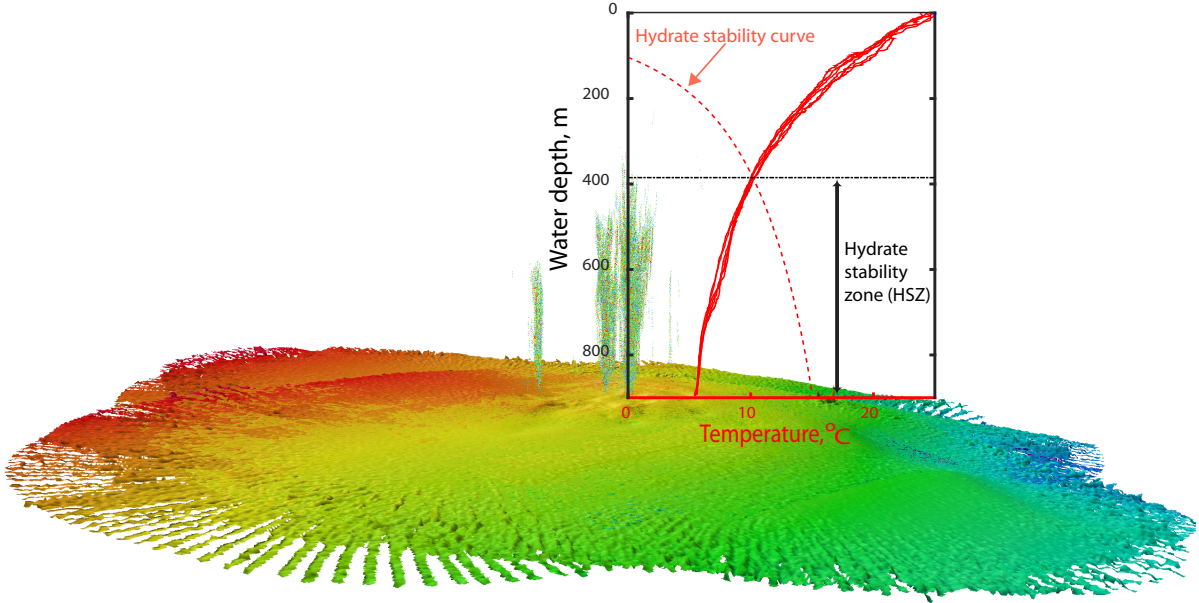


Figure 5: Image of the natural seep flare in the water column from post-processed EM-302 data together with the measured temperature profile and hydrate stability curve.

enough that the spatial extent of the plume changed with time so that the image at 190 m would have been for slightly different source conditions.

Our first analysis of the M3 sonar data is to extract the plume width as a function of height. The plume spreads out in the along-current direction due to sorting of the bubbles by the current. In the across-current direction, turbulent diffusion, bubble wobbling motion, and any plume entrainment is responsible for the plume spread. Figure 7 shows the evolution of the flare width in the cross-current direction with height for one dive during G08.

We noted by plotting the data in log space (not shown) that the plume width b grows with height z as $b \propto z^{1/2}$. Since the bubble rise velocity is virtually constant, this power law growth rate suggests a diffusion process is responsible for the plume growth and is in contrast to a power law of $b \propto z$, which would indicate an entraining plume growth rate (Fischer et al. 1979). To estimate the effective diffusion coefficient, we used the TAMOC model to simulate the random walk of 1000 bubbles sampled randomly from the bubble size distribution in Figure 2. The model considers dissolution and uses clean-bubble mass transfer rates until a hydrate formation time, after which dirty-bubble rates are used. The hydrate formation time is based on data from Rehder et al. (2009). The curves in Figure 7 show the model predicted plume width for different values of the effective diffusion coefficient. Values between $1 \cdot 10^{-4}$ and $5 \cdot 10^{-4}$ m²/s match most of the

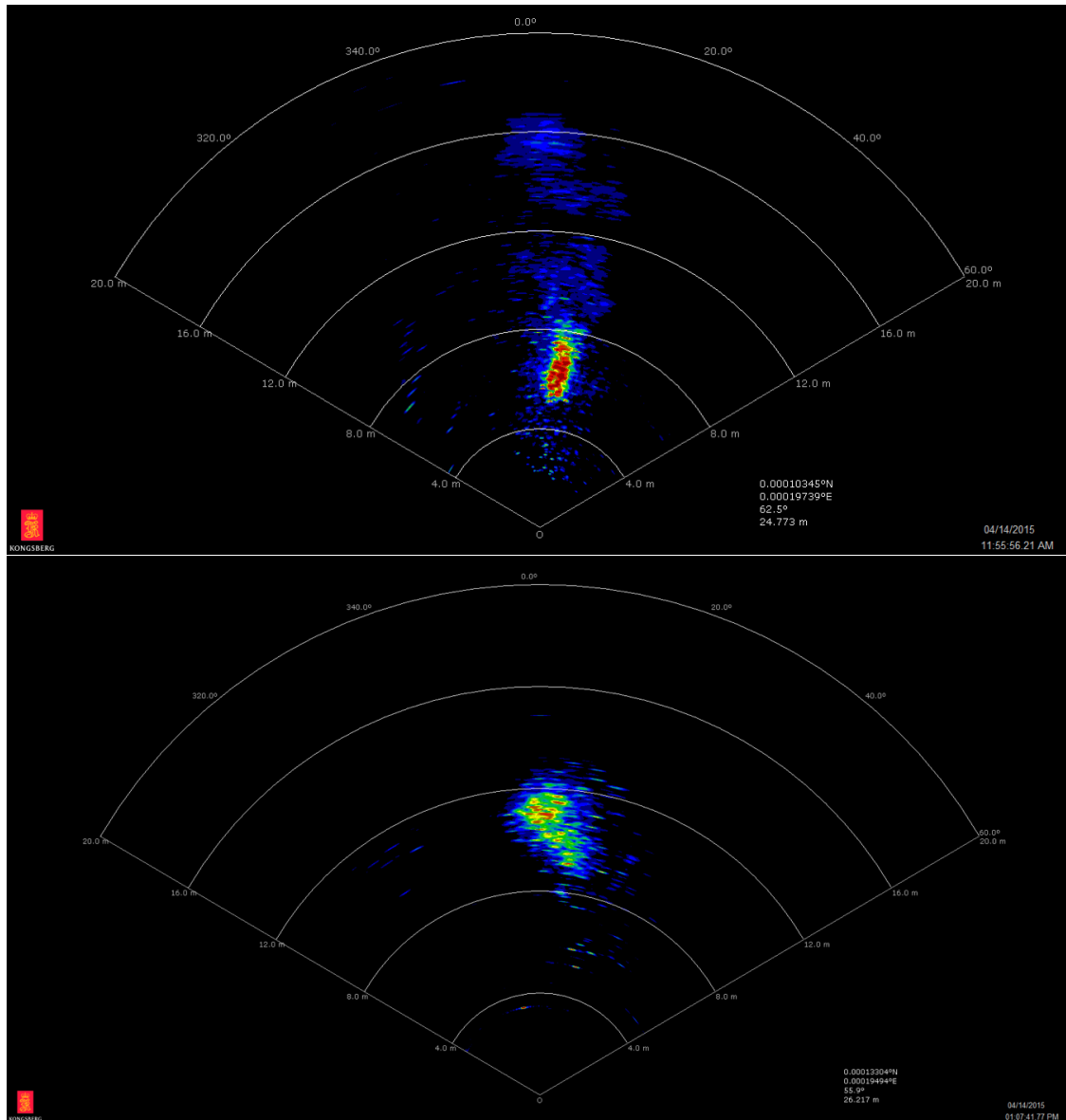


Figure 6: Two sample images recorded by the M3 Sonar during the GISR G08 Cruise. Upper panel: altitude 90 m; lower panel: altitude 190 m. The range for image plotted in both panels is 20 m.

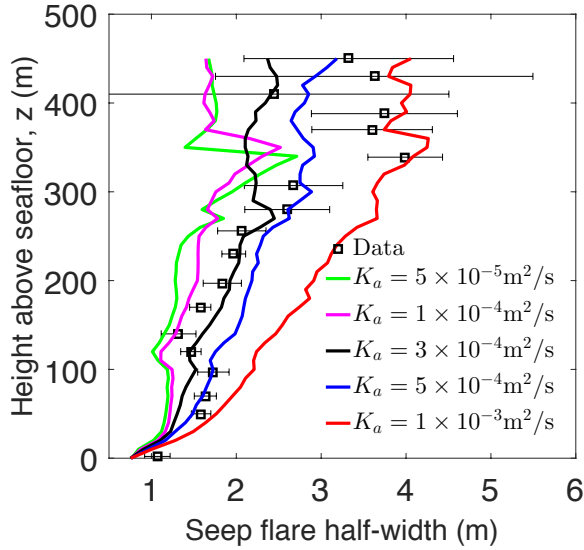


Figure 7: Width of seep flare plume from the M3 sonar for dive H1402. Measurement data were obtained from 50 Sonar images with errorbars reporting the standard deviation of the data. Model results from TAMOC for different lateral diffusivities are plotted, showing plume width given as 2σ , where σ is the standard deviation of modeled bubble locations at each altitude.

data, with some higher spreading observed in the data above 350 m altitude. This range of the apparent diffusion coefficient is in agreement with results from Okubo (1971) for ocean turbulence for diffusing clouds of size of order 1 m, similar to the size of our plume. Hence, we conclude that lateral ocean turbulent diffusion an important mechanism that spreads out the bubbles in the bubble flare. This also means that entrainment of ambient water and subsequent vertical transport in the bubble plume is a negligible process for these weak plumes subject to deep ocean currents.

Figure 8 shows the plume spreading measured by the M3 sonar for several dives during the G08 cruise with the model predictions for each dive. For the simulations, the bubbles are initialized using the measured bubble size distribution for each dive and ambient currents are obtained from a nearby acoustic doppler current profiler (ADCP) on a drill ship less than 1 km from the seep source. For most cases, the model and data are in good agreement. For Dive H1402, the greater spreading above 350 m altitude is likely associated with higher currents observed in that region during that dive; hence, the effective diffusion coefficient may also depend on the magnitude of the currents or the vertical velocity shear.

Progress Toward Milestone. The major milestone for Task 3 is to create a Matlab analysis program that can use the TAMOC model together with the acoustic data to infer bubble properties for bubbles observed in the acoustics. Our approach follows an approach by Weber et al. (2014),

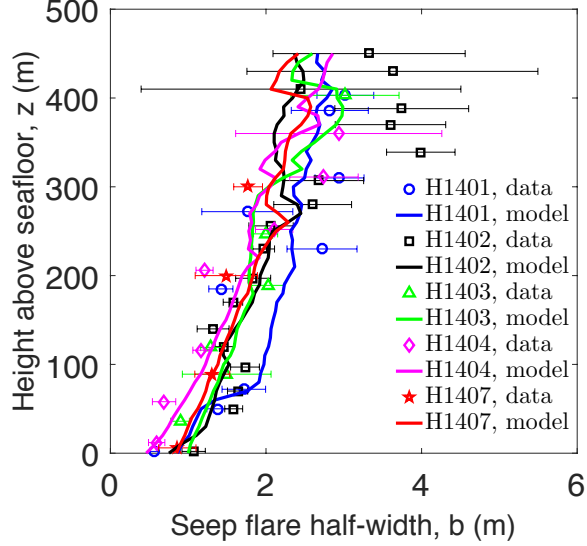


Figure 8: Comparison of bubble spreading between the model and measurements for all dives in G08. $K_a = 3 \times 10^{-4} \text{ m}^2/\text{s}$ is used in all simulations.

and we have started to develop our analysis code during the present reporting cycle.

Acoustic instruments measure backscatter intensity of sound reflected from objects in the water column. In the case of bubbles, the incoming acoustic signal excites the bubble-water interface, which then gives off a loud response, which is measured as backscatter by the multibeam transducer. Unfortunately, the backscatter depends on both the bubble size and the concentration of bubbles, so that bubble characteristics cannot be computed directly from single-frequency acoustic instruments (such as the M3 and EM-302). The approach by Weber et al. (2014) is to use a model, such as TAMOC, to predict the evolution of the bubble size, and then to infer the bubble concentration from the acoustic measurement using the predicted bubble size and the backscatter measurement.

In Figure 9 we show the acoustic backscatter of the M3 sonar (left column) together with the predicted backscatter from our acoustic model in Matlab using TAMOC results as input (right column). For the acoustic model, we use TAMOC to predict both the bubble size and concentration in the water column and then compute the theoretical acoustic backscatter that would be observed by an M3 sonar for those TAMOC-predicted characteristics. The figure shows that the magnitude and distribution of the model-predicted backscatter is similar to that measured by the M3 sonar. This demonstrates that 1.) our acoustic model gives similar backscatter prediction to that observed by the M3 and that 2.) TAMOC simulates the evolution of bubbles in the water column in a way that is similar to the observations.

While the M3 data yield cross-sections through the plume, the EM-302 data show the three-

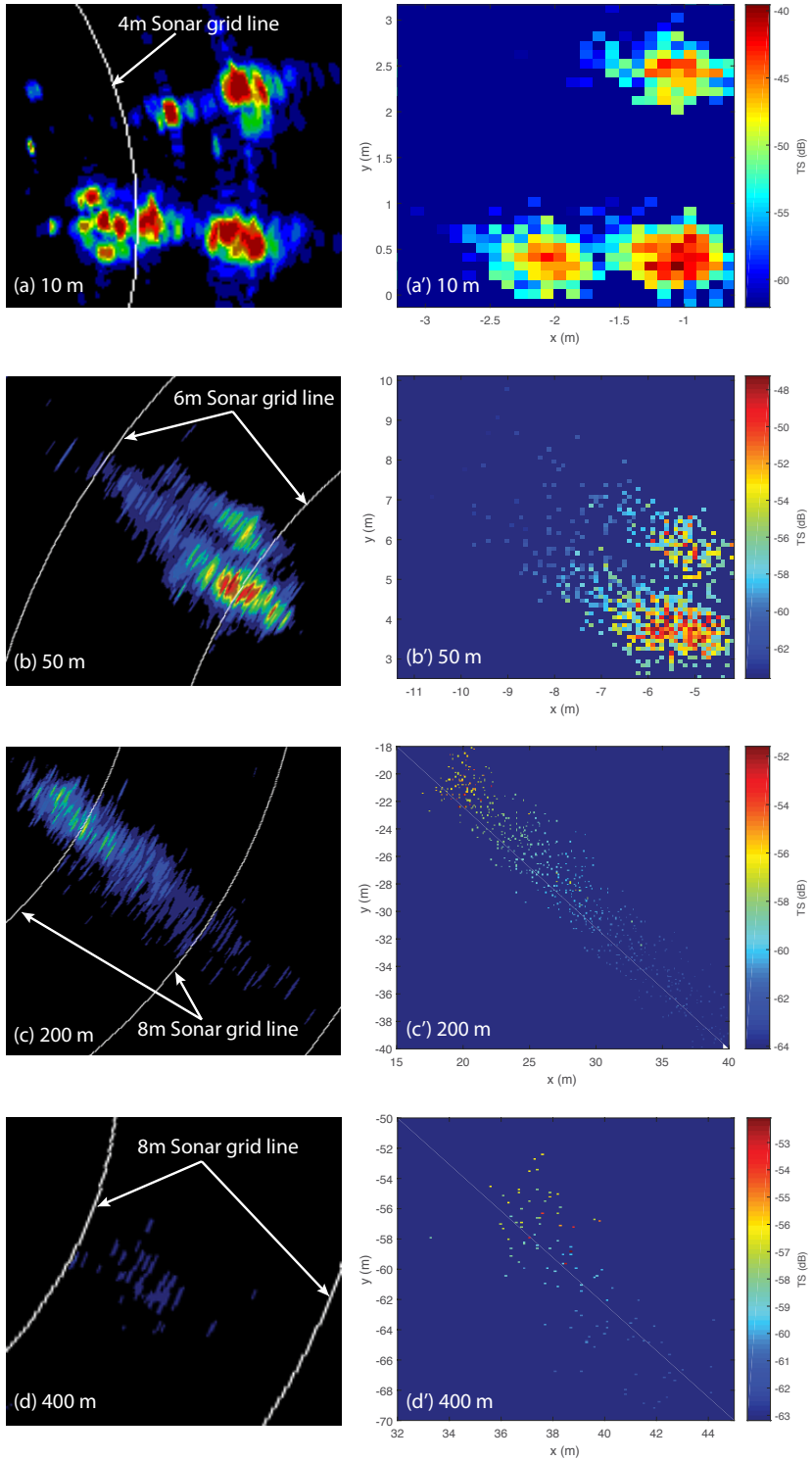


Figure 9: Comparison between the measured M3 sonar image (left column) and the target strength map created from the model result (right column).

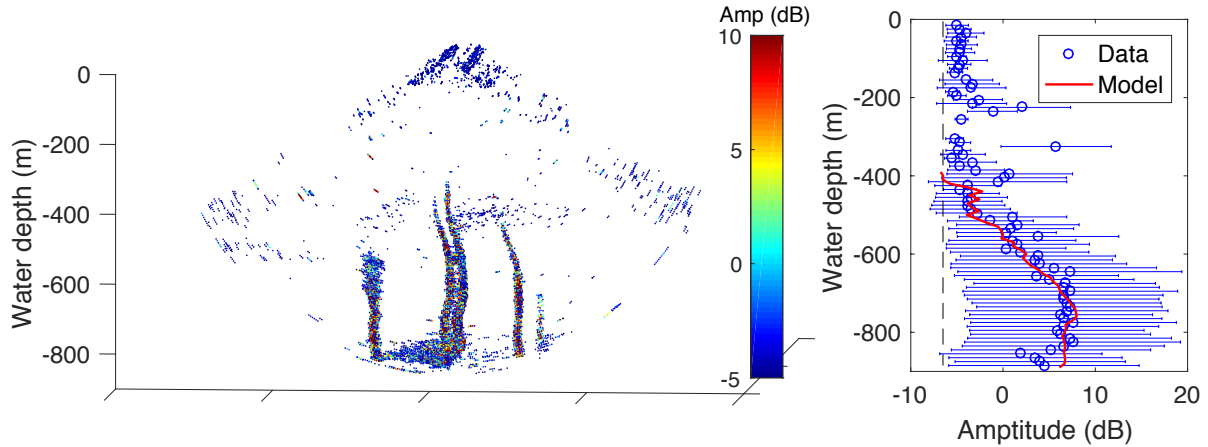


Figure 10: Left panel: 3-D scatter plot of unspecified amplitude from the EM-302 after noise removal, illustrating the location and magnitude of seep bubbles; right panel: comparison between the modeled target strength and the measured unspecified amplitude, where errorbars present standard deviation of the data, and dashed line shows the obtained noise level below which all data points were removed in the scatter plot. The model profile is offset by 17 dB to match the location of measured unspecified amplitude.

dimensional bubble flare in the water column. Figure 10 shows the raw data of the EM-302 (left and blue on right) with data predicted by our acoustic model for the EM-302 (red on right). This data-model comparison is similar to that in Figure 9: for the modeled data we take TAMOC output for bubble size and concentration and convert those predictions to acoustic backscatter using the theoretical backscattering model. Again, the model and the measurements show very good agreement in trends. However, the modeled acoustic backscatter must be offset by 17 dB in order to line up with the uncalibrated, raw data from the EM-302.

The next steps in the acoustic modeling will be to resolve differences in the magnitudes of the acoustic backscatter predicted by the model and measured by the instruments and to adapt our codes to use the acoustic data to predict concentration using bubble sizes modeled *via* TAMOC. The first of these steps will be the calibration phase of the acoustic modeling, and this will be supported by the *in situ* measurements from the camera so that we do not have to rely solely on predictions from the numerical model. The second step is a straightforward inversion of the theoretical acoustic equation. Hence, we have demonstrated that the acoustic data collected during the G08 cruise (and by inference also the G07 cruise) contain valuable information on the acoustic backscatter of these flares and that we are able to interpret these data using theoretical acoustic models. In the next quarter, we will continue to calibration the acoustic instruments and adapt our acoustic model to obtain data that can be used to validate TAMOC.

1.3 Deliverables

Two deliverables were completed during the present reporting period. These were:

1. **Project Management Plan (PMP)**. The PMP was delivered in its accepted and final form on October 28, 2016.
2. **Data Management Plan (DMP)**. No revisions were requested by the Project Officer to the plan submitted with the proposal; hence, the original DMP is the present guiding document. Revisions will be updated as necessary throughout the project as required by the Project Officer.

In the coming quarter, no new deliverables will be due.

1.4 Milestones Log

Table 1 presents the schedule of milestones with their verification methods for the duration of the project period. No milestones were due during the present reporting period. See Section 1.2 for details on progress toward completion of up-coming milestones.

1.5 Plans for the Next Reporting Period

Work for the next reporting period will continue on Tasks 2 and 3 (refer to Figure 1). For Task 2, we should complete collection of the NETL HPWT data by the end of January 2017, and work will continue to begin analyzing the HPWT data. The first task will be to catalog the data and adapt our Matlab image analysis programs to the images in the HPWT dataset.

For Task 3 we will begin building the complete observations database for both the G07 and G08 cruises and will continue post-processing of data from the G08 cruise. We will also continue development of our Matlab code to interpret the M3 and EM-302 data using our seep bubble model. Finally, we will begin a draft of a journal article to report the results of the G08 cruise. Our target journal for this article is *Geophysical Research Letters*.

References

- Clift, R., J. R. Grace, and M. E. Weber (1978), *Bubbles, drops, and particles*, Academic Press.
- Fisher, H. B., E. J. List, R. C. Y. Koh, J. Imberger, and N. H. Brooks (1979), *Mixing in inland and coastal waters*, Academic Press.

Table 1: Milestones schedule and verification methods.

	Milestone	Completion Date	Comments
Title	Acquisition of NETL HPWT data		
Planned Date	January 2017		
Verification Method	Report		
Title	Adapt Matlab code to NETL data		
Planned Date	September 2017		
Verification Method	Report		
Title	Matlab code for M3 and EM-302 data		
Planned Date	September 2017		
Verification Method	Report		
Title	OTRC Experimental Report		
Planned Date	August 2018		
Verification Method	Report		
Title	Adapt seep model to NETL data		
Planned Date	June 2018		
Verification Method	Report		
Title	Quantify seep model performance		
Planned Date	December 2018		
Verification Method	Report		
Title	Quantify performance of acoustic models		
Planned Date	March 2019		
Verification Method	Report		

- Okubo, A. (1971), Oceanic diffusion diagrams, *Deep Sea Research and Oceanographic Abstracts*, 18(8), 789–802.
- Rehder, G., I. Leifer, P. G. Brewer, G. Friederich, and E. T. Peltzer (2009), Controls on methane bubble dissolution inside and outside the hydrate stability field from open ocean field experiments and numerical modeling, *Marine Chemistry*, 114(1-2), 19–30.
- Wang, B., and S. A. Socolofsky (2015), A deep-sea, high-speed, stereoscopic imaging system for in situ measurement of natural seep bubble and droplet characteristics, *Deep Sea Research Part I*, 104, 134–148.
- Wang, B., S. A. Socolofsky, J. A. Breier, and J. S. Seewald (2016), Observation of bubbles in natural seep flares at MC 118 and GC 600 using in situ quantitative imaging, *Journal of Geophysical Research: Ocean*, 121, 2203–2230.
- Weber, T. C., L. Mayer, K. Jerram, J. Beaudoin, Y. Rzhhanov, and D. Lovalvo (2014), Acoustic estimates of methane gas flux from the seabed in a 6000 km² region in the northern gulf of mexico, *Geochemistry Geophysics Geosystems*, 15(5), 1911–1925.

2 Products

2.1 Publications, Conference Papers, and Presentations

The Project Kick-Off Presentation was made by Drs. Socolofsky and Wang via WebEx to DOE NETL on November 14, 2016. There are no other items to report.

2.2 Websites or Other Internet Sites

The natural seep model used for this project, the Texas A&M Oilspill Calculator (TAMOC), is published via an open source code sharing service at:

<http://github.com/socolofs/tamoc>

2.3 Technologies or Techniques

Nothing to report.

2.4 Inventions, Patent Applications, and/or Licenses

Nothing to report.

2.5 Other Products

Nothing to report.

3 Participants and other collaborating organizations

3.1 Project Personnel

- 1. **Name:** Scott A. Socolofsky
- 2. **Project Role:** Principal Investigator
- 3. **Nearest person months worked during reporting period:** 1
- 4. **Contribution to Project:** Overall project management and direction. Dr. Socolofsky has led the collection of the HPWT data and completed all project reporting requirements.
- 5. **Collaborated with individual in foreign country:** No

6. **Travelled to foreign country:** No

- 1. **Name:** Binbin Wang
- 2. **Project Role:** Co-Principal Investigator
- 3. **Nearest person months worked during reporting period:** 2
- 4. **Contribution to Project:** Analyzed the image data for the G08 cruise, created model for acoustic data from M3 sonar and EM-302 multibeam, and compared the measured data to model results from TAMOC.
- 5. **Collaborated with individual in foreign country:** No
- 6. **Travelled to foreign country:** No

3.2 Partner Organizations

None to report.

3.3 External Collaborators or Contacts

This project works in close collaboration with researchers in the DOE/NETL funded project “Fate of Methane in the Water Column,” led by the U.S. Geological Survey (USGS) in Woods Hole (Carolyn Ruppel), and with a new project led by the University of Rochester (John Kessler) to advance understanding of the environmental implications that methane leaking from dissociating gas hydrates could have on the ocean-atmosphere system. Dr. Socolofsky visits and communicates with researchers in these projects regularly and shares updates on work in progress. Accomplishments associated with these collaborations are detailed in Section 1.

4 Impact

None at this point.

5 Changes / Problems

Personnel. The project has been delayed in hiring the associated Ph.D. graduate student. This occurred because both the Funding Opportunity Announcement and the decision to fund this project occurred after the latest date to accept new graduate students for the fall 2016 semester

at Texas A&M University. As a result, recruitment of a new graduate student for the project had to focus on spring 2017 as a likely start date. Dr. Socolofsky posted a position announcement on his University website, and requested the help of colleagues both at Texas A&M and outside to help advertise the position. Two students applied directly for the position by November 2016. Dr. Socolofsky interviewed each student and followed up by requesting letters of recommendation. Dr. Socolofsky selected a new Ph.D. graduate student January 16, 2017, and has provided a start date of January 20, 2017. The new graduate student has completed all but two courses required for the Ph.D. degree and has a strong background in oceanography, data analysis, computer programming, modeling, ocean engineering, and fluid dynamics.

The project budget and schedule were both written with the understanding that it was unlikely a Ph.D. student could be found to start in the first quarter of the project. As a result, extra effort was budgeted for the Co-PI, Dr. Wang, and the project schedule calls for the Ph.D. student to catch up on coursework and learn the needed tools for the project under the direction of Dr. Wang throughout the first year of the project. It is fortunate that a suitable student could be identified at this early stage, and we conclude that the project is expected to continue on schedule. It is possible that a short no-cost extension will be requested to extend the project by one quarter if the Ph.D. student does not finish before December 2019.

Data. We initiated the process to obtain the NETL HPWT data as soon as the project budget was approved. Our initial plan was to transfer the data over FTP from NETL to Texas A&M. To accomplish this task, we purchased a network storage device (allocated in the project budget) and set up the necessary FTP server. There was some delay in overcoming firewalls, and the connection was established by early December 2016. After a few days of data transfer it became apparent that FTP transfer speeds were too slow for this volume of data. At that time, NETL curator of the data, Franklin Shaffer, began transferring the data to hard drives to send to Texas A&M University. The first set of drives arrived on January 7, 2017, and we began transferring data the week of January 8. It takes about one week to transfer the data from each set of four three-terabyte drives. Two of the drives in the first shipment were improperly encrypted, so a second set had to be copied. The final set of drives were sent January 13, 2017. As long as no more encrypted drives are encountered, we should have all of the data stored on our server by the end of January 2017. Our first milestone is due January 31, 2017, and requires us to have all of the data. While we are on-track to meet this deadline, if any of the drives need to be recopied and resent, we may miss the deadline by a few

days or a week. This should not adversely affect the overall project progress, and we are thankful to NETL and Franklin Shaffer for all of the effort he has given in making this data available to us in a timely fashion.

6 Special Reporting Requirements

None required.

7 Budgetary Information

Table 2 summarizes expenditures for the current phase of the project. The current, reported spending is lower than actual because the co-PI, Binbin Wang, could not immediately be charged to the project. His title changed at Texas A&M University, which required written permission from the project manager at DOE NETL to bill his time. The payroll correction paperwork has been filed, but his salary has yet to post to the project. After the payroll correction, project spending should be closer to being on track. This correction will be reflected in the second quarter budget report.

Table 2: Budget Report

Baseline Reporting Quarter	Budget Period 1							
	Q1		Q2		Q3		Q4	
	10/1/16 - 12/31/16		1/1/17 - 3/31/17		4/1/17 - 6/30/17		7/1/17 - 9/30/17	
DE-FE0028895	Q1	Cumulative Total	Q2	Cumulative Total	Q3	Cumulative Total	Q4	Cumulative Total
Baseline Cost Plan								
Federal Share	\$33,752	\$33,752	\$29,716	\$63,468	\$27,810	\$91,278	\$53,034	\$144,312
Non-Federal Share	\$12,029	\$12,029	\$12,029	\$24,058	\$8,019	\$32,077	\$4,009	\$36,086
Total Planned	\$45,781	\$45,781	\$41,745	\$87,526	\$35,829	\$123,355	\$57,043	\$180,398
Actual Incurred Cost								
Federal Share	\$11,037							
Non-Federal Share	\$12,029							
Total Incurred Costs	\$23,066							
Variance								
Federal Share	\$-22,715							
Non-Federal Share	\$0							
Total Variance	\$-22,715							